

FSU-HEP-931104
 SSCL-Preprint-531
 UH-511-777-93

DETECTING SLEPTONS AT HADRON COLLIDERS AND SUPERCOLLIDERS

Howard Baer¹, Chih-hao Chen¹, Frank Paige²
 and Xerxes Tata³

¹*Department of Physics, Florida State University, Tallahassee, FL 32306 USA*

²*Superconducting Supercollider Laboratory, Dallas, TX 75237 USA, and
 Brookhaven National Laboratory, Upton, NY 11973 USA*

³*Department of Physics and Astronomy, University of Hawaii, Honolulu, HI 96822 USA*

(July 26, 2018)

Abstract

We study the prospects for detecting the sleptons of the Minimal Supersymmetric Standard Model at hadron colliders and supercolliders. We use ISAJET 7.03 to simulate charged slepton and sneutrino pair production, incorporating slepton and sneutrino cascade decays into our analysis. We find that even with an accumulation of $\sim 1\text{fb}^{-1}$ of integrated luminosity, it will be very difficult to detect sleptons beyond the reach of LEP at the Fermilab Tevatron $p\bar{p}$ collider, due to a large background from W pair production. At LHC, sleptons of mass up to 300 GeV ought to be detectable via dilepton signal as long as it is possible to veto central jets with $p_T \geq 25$ GeV with high efficiency.

I. INTRODUCTION

It has long been known that supersymmetrization of the Standard Model (SM) leads to the stabilization of fundamental scalar masses, provided that super-partner masses are less than ~ 1 TeV [1]. More recently, it has been observed that the precision measurements of gauge couplings at scale M_Z by the LEP experiments are also consistent with the simplest supersymmetric grand unified model (but not with minimal SU(5)) if sparticle masses are ~ 1 TeV [2]. These motivations have prompted the recent re-examination of signatures for supersymmetry (SUSY) at various hadron colliders. Attention has been focussed mainly on the strongly interacting sparticles, squarks and gluinos [3], charginos and neutralinos [4], and Higgs bosons of SUSY [5].

In contrast, SUSY signals from slepton production at hadron colliders have received rather limited attention, probably due to the smallness of the cross sections. Early studies [6] were limited to slepton production via decays of real W and Z bosons at the CERN SppS Collider. Del Aguila and Ametller [7] have performed the most detailed study of these signals at hadron supercolliders and concluded that sleptons should be detectable with masses up to 250 GeV at the Large Hadron Collider (LHC) and up to 350 GeV at the unfortunately now defunct Superconducting Supercollider (SSC). To the best of our knowledge, there does not exist any analysis of slepton signals for the experiments at the Tevatron which are expected to accumulate a combined integrated luminosity of 100 pb^{-1} by the end of the current Tevatron Run 1B.

The purpose of this paper is to reexamine the prospects for detecting sleptons and sneutrinos at both the Fermilab Tevatron Collider and at LHC. We have improved on the analysis of Ref. [7] in several respects. Unlike these authors who assume that sleptons always directly decay to the LSP, we have incorporated all their cascade decay patterns. Generally speaking, these decays lead to reduction of the acollinear dilepton signal and are particularly important for the left-type sleptons. Also, we have used ISAJET 7.03 for our analysis, and so have a somewhat more realistic simulation of the signal and backgrounds as compared to previous analyses which were done at the parton level. This is especially important for the simulation of the extent of the hadronic activity in the signal events which, as we will see, will be useful in discriminating the signal from top quark background.

We work within the framework of the Minimal Supersymmetric Standard Model (MSSM) [1], which is the simplest supersymmetric extension of the SM. In the MSSM, for each generation of leptons (ν_ℓ, ℓ) , there exists two spin zero charged sleptons, $\tilde{\ell}_L$ and $\tilde{\ell}_R$, and a neutral spin zero particle, the sneutrino $\tilde{\nu}_L$. The mixing between charged sleptons is proportional to the corresponding *fermion* mass, and so, is completely negligible except possibly in the tau sector. Since we will mainly be concerned with the first two families of sleptons, we assume the L and R weak eigenstates are also the physical particles for the remainder of this paper.

Various experiments have already put lower bounds on slepton and sneutrino masses. The ASP Collaboration [8] which searched for single photon events produced via the reaction $e^+e^- \rightarrow \tilde{Z}_1\tilde{Z}_1\gamma$ has excluded selectrons with mass $m_{\tilde{e}} < 58$ GeV if L and R selectrons are degenerate, and \tilde{Z}_1 is a massless photino. This bound is sensitive to the composition of the LSP [9], and further, disappears if $m_{\tilde{Z}_1} > 12.5$ GeV. Non-observation of acoplanar dilepton plus missing energy events in the four LEP experiments [10] leads to the bounds,

$$\begin{aligned} m_{\tilde{\ell}_L} &> 45 \text{ GeV}, \\ m_{\tilde{\ell}_R} &> 45 \text{ GeV}, \end{aligned} \quad (1)$$

which are valid unless $m_{\tilde{Z}_1} \simeq m_{\tilde{\ell}}$. Constraints can also be placed on sneutrino masses at LEP, even though sneutrinos are expected to decay invisibly [11,10]. The combined LEP experiments require non-standard contributions to the Z boson invisible width to be $\Delta\Gamma_{\text{inv}} < 17$ MeV at 95% CL, which implies [10]

$$\begin{aligned} m_{\tilde{\nu}_L} &> 37 \text{ GeV (single sneutrino)}, \\ m_{\tilde{\nu}_L} &> 41.7 \text{ GeV (three degenerate sneutrinos)}. \end{aligned} \quad (2)$$

Our choices for sparticle masses and mixing angle parameters are guided by the framework of supergravity grand unified theories. In supergravity models, supersymmetry breaking leads to a common mass for sfermions at the unification scale. The degeneracy of sfermions present at the unification scale is broken when these masses are evolved down to the weak scale. Since the lepton masses are negligible, the slepton masses can then be written as [12],

$$m_{\tilde{\ell}_L}^2 = m_{\tilde{q}}^2 - 0.73m_{\tilde{g}}^2 - 0.27M_Z^2 \cos 2\beta, \quad (3a)$$

$$m_{\tilde{\ell}_R}^2 = m_{\tilde{q}}^2 - 0.78m_{\tilde{g}}^2 - 0.23M_Z^2 \cos 2\beta, \quad (3b)$$

$$m_{\tilde{\nu}_L}^2 = m_{\tilde{q}}^2 - 0.73m_{\tilde{g}}^2 + 0.5M_Z^2 \cos 2\beta, \quad (3c)$$

where $m_{\tilde{q}}^2$ is the squark mass squared averaged over all the flavours.

We see that for $m_{\tilde{q}} \gg m_{\tilde{g}}$, the squarks are basically degenerate with the sleptons; significant splitting between the masses of the three slepton types is possible only when squarks and gluinos are roughly degenerate, in which case, sleptons are considerably lighter than the squarks. For the convenience of the reader, we have plotted in Fig. 1 the various slepton masses as a function of $m_{\tilde{g}}$ where we take the average squark masses to be *a*) $m_{\tilde{q}} = m_{\tilde{g}}$, and *b*) $m_{\tilde{q}} = 2m_{\tilde{g}}$. We show results for $\tan\beta = 2$ and 20. Thus, from Fig. 1a, we see that if squark and gluino masses are nearly equal, there is an expected large splitting of the various slepton masses, with the sneutrino being the lightest slepton for low gluino masses, while $\tilde{\ell}_R$ is lightest for gluino masses larger than about 300 GeV. Furthermore, there is a large splitting between squark and slepton masses, with sleptons being considerably lighter than squarks. In this situation, the leptonic decays of neutralinos, and sometimes, also of charginos can be significantly enhanced [4]. Finally, we see from Fig. 1b, that if all the sleptons and the squarks (other than t -squarks which do not concern us here) are significantly heavier than gluinos, these must be essentially degenerate.

The rest of this paper is organized as follows. In Sec. 2, we discuss slepton production and decay at hadron colliders, and discuss details of our simulation. In Sec. 3, we investigate slepton signals and backgrounds relevant for Tevatron experiments, while in Sec. 4, we examine slepton signals and relevant backgrounds at the LHC. We conclude in Sec. 5 with a brief summary of our results.

II. SLEPTON PRODUCTION, DECAY AND SIMULATION

At hadron colliders, sleptons are dominantly pair-produced via Drell-Yan (DY) process mediated by a (virtual) W , γ or Z in the s -channel. The rate for slepton production via

WW [13] or gg fusion [7] processes is smaller by at least an order of magnitude at the LHC and is entirely negligible at Tevatron energies. Sleptons can also be singly produced via decays of charginos or neutralinos produced by the cascade decays of squarks and gluinos. Since such events will be difficult to sort out from other cascade decay patterns of gluinos and squarks [3,14], we will focus on direct slepton production via the DY mechanism in this paper.

The cross section for the production of charged slepton-sneutrino pairs is given by

$$\frac{d\sigma}{dt}(d\bar{u} \rightarrow W \rightarrow \tilde{\ell}_L \bar{\nu}_L) = \frac{g^4 |D_W(\hat{s})|^2}{192\pi \hat{s}^2} (\hat{t}\hat{u} - m_{\tilde{\ell}_L}^2 m_{\bar{\nu}_L}^2). \quad (4)$$

For $\tilde{\ell}_L$ pair production, the cross section is given by [15]

$$\begin{aligned} \frac{d\sigma}{dt}(q\bar{q} \rightarrow \gamma^*, Z \rightarrow \tilde{\ell}_L \bar{\tilde{\ell}}_L) &= \frac{e^4}{24\pi \hat{s}^2} (\hat{t}\hat{u} - m_{\tilde{\ell}_L}^4) \\ &\times \left\{ \frac{q_\ell^2 q_q^2}{\hat{s}^2} + (\alpha_\ell - \beta_\ell)^2 (\alpha_q^2 + \beta_q^2) |D_Z(\hat{s})|^2 + \frac{2q_\ell q_q \alpha_q (\alpha_\ell - \beta_\ell) (\hat{s} - M_Z^2)}{\hat{s}} |D_Z(\hat{s})|^2 \right\}, \end{aligned} \quad (5)$$

where $D_V(\hat{s}) = 1/(\hat{s} - M_V^2 + iM_V\Gamma_V)$ and the α 's, β 's, and charge assignments q are given in Ref. [16]. The cross section for sneutrino pair production can be obtained by replacing α_ℓ , β_ℓ , q_ℓ and $m_{\tilde{\ell}}$ by α_ν , β_ν , 0 and $m_{\tilde{\nu}}$, respectively, whereas for $\tilde{\ell}_R$ pair production one substitutes $\alpha_\ell - \beta_\ell \rightarrow \alpha_\ell + \beta_\ell$, and $m_{\tilde{\ell}_L} \rightarrow m_{\tilde{\ell}_R}$ in Eq.(5).

The left-sleptons dominantly decay via gauge interactions into charginos or neutralinos via the (kinematically accessible) two body decays,

$$\begin{aligned} \tilde{\ell}_L &\rightarrow \ell + \tilde{Z}_i, \\ \tilde{\ell}_L &\rightarrow \nu_\ell + \tilde{W}_j. \end{aligned} \quad (6)$$

and

$$\begin{aligned} \tilde{\nu}_L &\rightarrow \nu_\ell + \tilde{Z}_i, \\ \tilde{\nu}_L &\rightarrow \ell + \tilde{W}_j. \end{aligned} \quad (7)$$

If the sleptons are relatively light, only the decay to the LSP may be possible, so that a light sneutrino decays invisibly. Heavier sleptons, can also decay via the chargino or other neutralino modes. Unless suppressed by phase space these decays are important and, because they proceed via the larger $SU(2)$ gauge coupling, frequently dominate the direct decay to the LSP. The daughter charginos and neutralinos further decay until the cascade terminates in the stable LSP (\tilde{Z}_1).

In contrast, the $SU(2)$ singlet charged sleptons $\tilde{\ell}_R$ only decay via their $U(1)$ gauge interactions, so that in the limit of vanishing lepton Yukawa coupling their decays to charginos are forbidden. These thus decay via,

$$\tilde{\ell}_R \rightarrow \ell + \tilde{Z}_i, \quad (8)$$

Frequently, the branching fraction for the $\tilde{\ell}_R \rightarrow \ell \tilde{Z}_1$ mode is large even for rather high values of $m_{\tilde{\ell}_R}$; these decays are, therefore, a potential source of very hard isolated leptons at hadron

colliders. The dependence of the branching fractions for the various decays of sleptons and sneutrinos on the MSSM parameters has been studied in Ref. [17] to which we refer the reader.

The slepton production processes and decay modes discussed above have all been incorporated into the simulation program ISAJET 7.03 [18]. Briefly, for a given input parameter set ($m_{\tilde{g}}, m_{\tilde{q}}, m_{\tilde{\ell}_L}, m_{\tilde{\ell}_R}, m_{\tilde{\nu}_L}, \mu, \tan \beta, m_A$), the routine ISASUSY calculates all sparticle masses and branching fractions to various decay modes. ISAJET then produces slepton pairs according to probabilities given by the above production formulae convoluted with EHLQ Set 1 structure functions [19]. These sleptons then decay via the various cascades with appropriate branching fractions as given by the MSSM. Radiation of initial and final state partons is also included in ISAJET. Final state quarks and gluons are hadronized, and unstable particles are decayed until stable final states are reached. Underlying event activity is also modeled in our simulation.

III. SLEPTONS AT THE FERMILAB TEVATRON COLLIDER

The total DY production cross sections for slepton pairs via $p\bar{p}$ collisions at Tevatron collider energy $\sqrt{s} = 1.8$ TeV is shown in Fig. 2 as a function of slepton mass. On account of the LEP constraints, slepton production can only occur via off-shell W or Z exchanges, and so, each individual production cross section is typically below the 1 pb level. However, summing over the four processes shown, as well as summing over the e and μ families, can push the total slepton cross section above the pb level.

The dominant production cross section comes from $W^* \rightarrow \tilde{\ell}\tilde{\nu}_L$. Unless the sneutrino is heavier than the chargino or the \tilde{Z}_2 , it will decay invisibly via $\tilde{\nu} \rightarrow \nu \tilde{Z}_1$. Since the dominant decays of the selectron are $\tilde{\ell}_L \rightarrow \ell \tilde{Z}_1$, or if allowed, $\tilde{\ell}_L \rightarrow \tilde{W}_1 \nu_\ell$, the W^* production mode will result in single-hard-isolated-lepton plus missing energy events. Such event topologies have large backgrounds due to direct $W \rightarrow \ell\nu$ and $W \rightarrow \tau \rightarrow \ell$ decays, where ℓ can be either e or μ . Similarly, $Z^* \rightarrow \tilde{\nu}_L \tilde{\nu}_L$ will lead usually to little observable activity in the final state, and is not a promising search mode if sneutrino decays to the chargino are forbidden. The modes $\gamma^*, Z^* \rightarrow \tilde{\ell}_L \tilde{\ell}_L$ or $\tilde{\ell}_R \tilde{\ell}_R$ followed by each slepton decaying via $\tilde{\ell} \rightarrow \ell \tilde{Z}_1$ can lead to acollinear, hard isolated dilepton plus missing energy events with little jet activity, which constitutes the most promising signature for Tevatron collider searches. Backgrounds to the dilepton signature come from W pair production, from $t\bar{t}$ production, and from $Z \rightarrow \tau\bar{\tau}$ production. It should be remembered that the decay $\tilde{\nu}_L \rightarrow \tilde{W}_1 \ell$ rapidly dominates sneutrino decays when it is kinematically allowed; in this case sneutrino production is an additional source of acollinear dilepton pairs at the Tevatron.

In addition, there could be other SUSY processes which mimic this dilepton signature, for instance, DY production of chargino pairs, $\gamma^*, Z^* \rightarrow \tilde{W}_1 \tilde{W}_1$, followed by $\tilde{W}_1 \rightarrow \ell \nu_\ell \tilde{Z}_1$ decays. Dilepton events can also come from gluino and squark pair production [3], but these events should be accompanied by substantial jet activity.

To assess slepton detection prospects at the Tevatron collider, we simulated two cases of slepton production: we take

$$\text{Case 1: } m_{\tilde{g}} = m_{\tilde{q}} = -\mu = 150 \text{ GeV}, \tan \beta = 2$$

$$\text{Case 2: } m_{\tilde{g}} = m_{\tilde{q}} = -\mu = 200 \text{ GeV}, \tan \beta = 2$$

The above parameters are consistent with predictions from supergravity GUT models with radiative electroweak symmetry breaking [20]. The corresponding slepton masses can be read off Fig. 1a, and are listed in Table I as well. Case 1 leads to a somewhat lighter sparticle spectrum than case 2. In fact, it is very close to the region of parameter space excluded by the CDF [21] experiment from their analysis of the \cancel{E}_T data sample. We have shown it to illustrate the difficulty of detecting sleptons even when the sparticles are relatively light.

We use the toy calorimeter simulation package ISAPLT to model detector effects. We simulate calorimetry with cell size $\Delta\eta \times \Delta\phi = 0.1 \times 0.1$, which extends between $-4 < \eta < 4$ in pseudorapidity. We take hadronic (electromagnetic) energy resolution to be $70\%/\sqrt{E_T}$ ($15\%/\sqrt{E_T}$). Jets are coalesced within cones of $R = \sqrt{\Delta\eta^2 + \Delta\phi^2} = 0.7$ using the ISAJET routine GETJET. Clusters with $E_T > 15$ GeV are labelled as jets. Muons and electrons are classified as isolated if they have $p_T > 10$ GeV, $|\eta(\ell)| < 3$, and the visible activity within a cone of $R = 0.4$ about the lepton direction is less than $E_T(\text{cone}) = 5$ GeV.

We then impose the following cuts designed to select signal events, while vetoing SM backgrounds from W pair, $\tau\bar{\tau}$ and top quark pair production:

- require *two* isolated same flavor leptons with $p_T(\ell) > 15$ GeV,
- require missing transverse energy $\cancel{E}_T > 20$ GeV,
- require number of jets $n(\text{jets}) = 0$,
- require transverse opening angle $30^\circ < \Delta\phi(\ell\bar{\ell}) < 150^\circ$.

Cross sections after these cuts are listed in Table I in femtobarns. The dominant SM background with $m_t = 150$ GeV comes from WW production. No events from $t\bar{t}$ or $\tau\bar{\tau}$ production passed our cuts, yielding upper limits on background from these sources. The $t\bar{t}$ background estimate may be somewhat optimistic since we have assumed an idealized calorimeter covering $|\eta| < 4$ to determine the rejection from the jet veto.

After the collection of 1 fb^{-1} of data, we see that Case 1 would yield a cross-section at the 3σ level above WW background, while Case 2 is only 1.5σ above background. Of course, related processes such as chargino pair production also yield signal events, and could be factored in either as signal or background. Chargino pair rates for case 1 and 2 are listed in Table I as well for comparison. In Case 1, approximately $2/3$ of the slepton signal events come from $\tilde{\ell}_R\tilde{\ell}_R$ production, while the other $\sim 1/3$ comes from $\tilde{\ell}_L\tilde{\ell}_L$; sneutrinos make a negligible contribution. However, for Case 2, dileptons come nearly equally from RR and LL production, although now the LL component contains a substantial contribution from sneutrino pair production.

Since WW production leads to an equal number of $e\mu$ events (using the above cuts), it might be possible to compare the rate for $e\bar{e}$ and $\mu\bar{\mu}$ production to the rate for $e\bar{\mu} + \bar{e}\mu$ production. Evaluating $R = N(e\bar{e} + \mu\bar{\mu})/N(e\bar{\mu} + \bar{e}\mu)$ for integrated luminosity of 1 fb^{-1} yields in Case 1, $R = 1.4 \pm 0.3$, and in Case 2, $R = 1.25 \pm 0.25$, *i.e.* only a one standard deviation effect. Incorporation of more realistic detector effects and efficiencies would surely reduce these rates, leading us to conclude that detection of a slepton signal at the Tevatron collider would be extremely difficult.

IV. SLEPTON SEARCH AT THE LHC

The higher energy and higher luminosity available at the LHC will considerably enhance slepton production rates relative to the Tevatron, and leads to the possibility of detecting sleptons beyond the reach of LEP 200. In Fig. 3, we plot the slepton and sneutrino pair production cross sections at $\sqrt{s} = 14$ TeV (LHC), once again using EHLQ Set 1 structure functions. For a design luminosity of $3 \times 10^4 \text{ pb}^{-1}/\text{yr}$, we see that at LHC, for instance, $pp \rightarrow \ell_R \bar{\ell}_R X$ can result in about 2400 (12) events annually for $m_{\tilde{\ell}_R} = 100$ (400) GeV. Summing over L and R slepton types, flavors and generations considerably enhances these rates.

For masses in the 100-400 GeV range, the cascade decays of sleptons are very important, and can lead to final states containing many isolated leptons and jets. We consider first the same-flavor isolated dilepton signature, then turn to the assessment of single lepton and other multi-lepton signatures.

To examine the possibility of detecting sleptons at the LHC, we examine four cases:

Case 3: $m_{\tilde{g}} = m_{\tilde{q}} = -\mu = 200$ GeV, $\tan \beta = 2$

Case 4: $m_{\tilde{g}} = m_{\tilde{q}} = -\mu = 400$ GeV, $\tan \beta = 2$

Case 5: $m_{\tilde{g}} = m_{\tilde{q}} = -\mu = 600$ GeV, $\tan \beta = 2$

Case 6: $m_{\tilde{g}} = m_{\tilde{q}} = -\mu = 800$ GeV, $\tan \beta = 2$,

for which slepton masses are ~ 100 , 200 , 300 and 400 GeV, respectively. Exact slepton and sneutrino masses may be read off Fig. 1a.

For LHC, we again use the toy calorimeter simulation package ISAPLT. We simulate calorimetry with cell size $\Delta\eta \times \Delta\phi = 0.05 \times 0.05$, which extends between $-5.5 < \eta < 5.5$. We take hadronic energy resolution to be $50\%/\sqrt{E_T}$ for $|\eta| < 3$, and to be a constant 10% for $3 < |\eta| < 5.5$, to model the effective p_T resolution of the forward calorimeter including the effects of shower spreading.

We take electromagnetic resolution to be $15\%/\sqrt{E_T}$. Jets are coalesced within cones of $R = \sqrt{\Delta\eta^2 + \Delta\phi^2} = 0.7$ using the ISAJET routine GETJET. For the purpose of jet veto (essential to eliminate top quark background), clusters with $E_T > 25$ GeV are labelled as jets. Muons and electrons are classified as isolated if they have $p_T > 20$ GeV, $|\eta(\ell)| < 2.5$, and the visible activity within a cone of $R = 0.3$ about the lepton direction is less than $E_T(\text{cone}) = 5$ GeV.

A. Dilepton signature at the LHC

For each of the four cases above, we generated 5000 slepton and sneutrino events in the ratio expected in the MSSM, and examined backgrounds from WW (50K events) and $t\bar{t}$ with $m_t = 150$ GeV (1.3M events). The background events have been forced to have primary leptonic decays. Unlike at the Tevatron, the major background at the LHC comes from $t\bar{t}$ production, and has a cross section of about 1500 pb for our choice of top mass.

To detect hard, isolated dilepton events, we impose the following cuts:

- A. require *two* isolated same flavor leptons, each with $p_T(\ell) > 20$ GeV,
- B. require missing transverse energy $\cancel{E}_T > 100$ GeV,
- C. require number of jets with $|\eta| < 3$ to be $n(jets) = 0$ (central jet veto),
- D. require transverse opening angle $\Delta\phi(\vec{p}_T(\ell\bar{\ell}'), \cancel{E}_T) > 160^\circ$,

and

- E. make a slepton mass dependent cut on $p_T(\ell) > p_{T_c}$, and $\Delta\phi(\ell\bar{\ell}') < \phi_c$, which we optimize (as discussed below) depending on the slepton mass.

The cross section after each cut is listed in Table II, along with the per cent of cross section that was cut. Cut A is more severe for background than for signal in part because it selects out the leptonic branching fractions, which are smaller for the background processes. As might be anticipated, the efficiency of cut B (\cancel{E}_T cut) is sensitively dependent on slepton mass, since higher mass sleptons yield a harder \cancel{E}_T spectrum. Cut C, the central jet veto, is very effective at cutting out $t\bar{t}$ events, since the auxiliary b -jets are frequently hard and central. Cut D is an additional cut designed to eliminate some fraction of $t\bar{t}$ events with soft b -jets; these jets, which fail to pass the jet requirements, affect the direction of the leptons and the \cancel{E}_T vector.

Finally, for cut E (high $p_T(\ell)$ and dilepton opening angle cut), we examined a matrix of p_{T_c} and ϕ_c values to find optimal signal to background levels. Results are given in Table III. We find that the choice $(p_{T_c}, \phi_c) = (40 \text{ GeV}, 90^\circ) [(80 \text{ GeV}, 140^\circ)]$ works well for the case of relatively light [heavy] sleptons. For the transition region around $m_{\tilde{\ell}} = 200$ GeV, we exhibit the results with both sets of cuts in Table III. When we found zero events in our simulation, we have used the 1 event level to represent the bound on the cross section. Such stringent cuts reduce the $t\bar{t}$ background to less than or equal to two events per year, whereas signal cross sections range from 66 (for case 3) to only 3 events (for case 6) per year.

As noted in Sec. 3, chargino pair production, followed by the leptonic decays of charginos may well mimic this dilepton signal. In order to get an idea of whether chargino production might be confused with slepton production, we generated chargino pair events with parameters as in cases 3 and 4 introduced above, and found that no events passed the cuts (A-E). This leads to an upper limit of 0.1 fb [0.03 fb] for case 3 [case 4] so that at least for these supergravity motivated parameter choices, the chargino signal is unlikely to be confused with that of the slepton. The reason for this is, of course, the very different kinematics in chargino and slepton events. We expect that the chargino background in cases 5 and 6 will be even smaller.

The crucial cut for the detectability of sleptons over the background from $t\bar{t}$ production is clearly the central jet veto. The results presented above assume 100% jet detection efficiency, whereas real detectors have regions of dead space. Without doing a real detector simulation, we estimated the $t\bar{t}$ background assuming a 99% jet detection efficiency. In this case, some $t\bar{t} \rightarrow \ell\bar{\ell} + 1$ -jet events could be mistaken for $\ell\bar{\ell} + 0$ -jet events. We list the background for this imperfect detector in column 7 of Table III, and see that in this case the background, though still smaller than the signal, is certainly relevant in that it may considerably degrade the statistical significance of any observed signal.

B. Other Leptonic Signals

Slepton production can also lead to other event topologies. The single lepton signal, from $W^* \rightarrow \tilde{\ell}_L \tilde{\nu}_\ell$ decays, is frequently larger than the dilepton signal discussed above. There are, however, several SM sources which can lead to this event topology. In Ref. [7] it has already been noted that the background from $pp \rightarrow WZ \rightarrow l\nu + \nu\nu$ production is comparable to the slepton signal. The dominant background, however, comes from single W production. It might be expected that in this case, the transverse mass $M_T(l, \cancel{E}_T)$ peaks sharply at M_W , while the signal exhibits a broad distribution. Toward this end, we have plotted, in Fig. 4, this distribution from the signal in cases 3 and 4, and also from W^* , WZ and $t\bar{t}$ production as given by the SM. We have required $\cancel{E}_T \geq 100$ GeV, $p_T(\ell) > 20$ GeV, and $n(\text{jets}) = 0$. The transverse mass distribution from W events do not exhibit the familiar Jacobian peak because the hard \cancel{E}_T requirement we have imposed selects out background mainly from off-shell W 's. We see that over the entire range of M_T where the signal is significant, it is swamped by the single W^* background. We thus conclude that detection of the slepton signal in this channel would be extremely difficult.

Another possible strategy might be to examine the hadronically quiet trilepton signal from the cascade decays of the sleptons. We have done so for each of the four LHC cases, and found no such events in our simulation in cases 5 and 6. In cases 3 and 4, we find signal cross sections of 4 fb and 1 fb, respectively; however, the corresponding cross sections from $\tilde{W}_1 \tilde{Z}_2$ production are 24 fb and 34 fb. We thus conclude that it is unlikely that trileptons from slepton sources will be detectable above those from chargino-neutralino associated production even if these signals are detectable above SM backgrounds [22].

V. SUMMARY AND CONCLUDING REMARKS

We have studied the prospects for detecting sleptons of supersymmetry, both at the Tevatron and at the proposed LHC. We find that the most promising signal consists of events with acollinear leptons and no jets. At the Tevatron, W pair production is the dominant background, while $t\bar{t}$ events, where the b jets are too soft to be detected, is the main background at the LHC. We have simulated the signal as well as these backgrounds using ISAJET 7.03 with suitable cuts to model the experimental conditions.

The signal cross sections we find are summarized in Tables I-III. We see from Table I that even with an integrated luminosity of 1 fb^{-1} , the slepton signal is at most 50% of the WW background for the cases we considered (the first of which has been picked to be nearly optimal within the constraints of supergravity models). Incorporation of realistic detector effects (such as cracks and imperfect electronics) would certainly reduce the signal. We thus conclude that the detection of sleptons at the Tevatron would be very difficult.

The situation is somewhat different for the LHC, where the higher energy and the high design luminosity enables us to make strong cuts to enhance the slepton signal over the background. We have designed two sets of cuts, one each for sleptons lighter/heavier than about 200 GeV. The signal cross sections after these cuts are shown in Table III together with the corresponding cross sections from the $t\bar{t}$ and WW backgrounds. We find that sleptons lighter than 200 GeV should be readily detectable with a year of LHC running at its design luminosity. With the cuts designed for detection of heavier sleptons, we see

that the signal is extremely small (with no background in our simulation) so that only a handful of events may be anticipated. We should also warn the reader that this conclusion is based on the assumption that the efficiency for jet detection is 100%. If this falls by more than 1%, backgrounds from top quarks can become significant, so that the detectability of heavy sleptons may be marginal. Finally, we have also examined other channels for slepton detection. We find that the single lepton channel is swamped by $W^* \rightarrow \ell \bar{\nu}$ events, whereas the rate for hadronically quiet trilepton events coming from the cascade decays of sleptons is dwarfed by that from direct $\tilde{W}_1 \tilde{Z}_2$ production. We also remark that we have limited our attention to a strongly correlated set of input SUSY parameters typical of supergravity models; breaking these correlations could lead to a modification of our conclusions concerning slepton detection at hadron colliders.

To summarize, we are pessimistic about the prospects for detecting the sleptons of supergravity at the Fermilab Tevatron. At the LHC, sleptons with masses up to 200-250 GeV should be readily detectable with a year of running at the design luminosity. Heavier sleptons might be also be detectable, but this would crucially depend on the efficiency for vetoing events with central jets.

ACKNOWLEDGMENTS

This research was supported in part by the U. S. Department of Energy under contract number DE-FG05-87ER40319, DE-AC35-89ER40486, and DE-AM03-76SF00235. In addition, the work of HB was supported by the TNRLC SSC Fellowship program.

REFERENCES

- [1] For a review of the MSSM, see H. P. Nilles, *Phys. Rep.* **110**, 1 (1984); P. Nath, R. Arnowitt and A. Chamseddine, *Applied $N = 1$ Supergravity*, ICTP Series in Theoretical Physics, Vol. I, World Scientific (1984); H. Haber and G. Kane, *Phys. Rep.* **117**, 75 (1985); X. Tata, in *The Standard Model and Beyond*, p. 304, edited by J. E. Kim, World Scientific (1991).
- [2] U. Amaldi, W. de Boer and H. Furstenau, *Phys. Lett.* **B260**, 447 (1991); J. Ellis, S. Kelley and D. Nanopoulos, *Phys. Lett.* **B260**, 131 (1991); P. Langacker and M. Luo, *Phys. Rev.* **D44**, 817 (1991).
- [3] H. Baer, C. Kao and X. Tata, *Phys. Rev.* **D48**, R2978 (1993).
- [4] H. Baer and X. Tata, *Phys. Rev.* **D47**, 2739 (1993); J. Lopez, D. Nanopoulos, X. Wang and A. Zichichi, *Phys. Rev.* **D48**, 2062 (1993); H. Baer, C. Kao and X. Tata, *Phys. Rev. D* (in press).
- [5] H. Baer, M. Bisset, C. Kao and X. Tata, *Phys. Rev.* **D46**, 1067 (1992); J. Gunion and L. Orr, *Phys. Rev.* **D46**, 2052 (1992); V. Barger, M. Berger, A. Stange and R. Phillips, *Phys. Rev.* **D45**, 4128 (1992); Z. Kunszt and F. Zwirner, *Nucl. Phys.* **B385**, 3 (1992).
- [6] R. M. Barnett, H. E. Haber and K. Lackner, *Phys. Rev. Lett.* **51**, 176 (1983); H. Baer, J. Ellis, D. Nanopoulos and X. Tata, *Phys. Lett.* **B153**, 265 (1985).
- [7] F. del Aguila and Ll. Ametller, *Phys. Lett.* **B261**, 326 (1991).
- [8] C. Hearty *et. al.*, (ASP Collaboration), *Phys. Rev.* **D39**, 3207 (1989) and references therein.
- [9] M. Drees, C-S. Kim and X. Tata, *Phys. Rev.* **D37**, 784 (1988).
- [10] D. Decamp *et. al.* (ALEPH Collaboration), *Phys. Lett.* **B236**, 86 (1990); P. Abreu *et. al.* (DELPHI Collaboration), *Phys. Lett.* **B247**, 157 (1990); B. Adeva *et. al.* (L3 Collaboration), *Phys. Lett.* **B233**, 530 (1989); M. Akrawy *et. al.* (OPAL Collaboration), *Phys. Lett.* **B240**, 261 (1990); for a review, and sneutrino limits, see G. Giacomelli and P. Giacomelli, CERN-PPE/93-107 (1993).
- [11] H. Baer, M. Drees and X. Tata, *Phys. Rev.* **D41**, 3414 (1990).
- [12] See *e.g.*, L. Ibanez and C. Lopez, *Nucl. Phys.* **B233**, 511 (1984); L. Hall and J. Polchinski, *Phys. Lett.* **B152**, 335 (1985); for an update, see *e.g.* M. Drees and N. Nojiri, *Nucl. Phys.* **B369**, 54 (1992).
- [13] J. Gunion, M. Herrero and A. Mendez, *Phys. Rev.* **D37**, 2533 (1988).
- [14] H. Baer, X. Tata and J. Woodside, *Phys. Rev.* **D45**, 142 (1992).
- [15] S. Dawson, E. Eichten and C. Quigg, *Phys. Rev.* **D31**, 1581 (1985).
- [16] M. Chen, C. Dionisi, M. Martinez and X. Tata, *Phys. Rep.* **159**, 201 (1988).
- [17] H. Baer, A. Bartl, D. Karatas, W. Majerotto and X. Tata, *Int. J. Mod. Phys.* **A4**, 4111 (1989).
- [18] F. Paige and S. Protopopescu, in *Supercollider Physics*, p. 41, ed. D. Soper (World Scientific, 1986); H. Baer, F. Paige, S. Protopopescu and X. Tata, FSU-HEP-930329 (1993), to appear in *Proceedings of the Workshop on Physics at Current Accelerators and the Supercollider*, ed. J. Hewett, A. White and D. Zeppenfeld, (World Scientific, 1993).
- [19] E. Eichten, I. Hinchliffe, K. Lane and C. Quigg, *Rev. Mod. Phys.* **56**, 759 (1984).
- [20] R. Arnowitt and P. Nath, private communication.
- [21] F. Abe *et. al.* *Phys. Rev. Lett.* **69**, 3439 (1992).

- [22] R. Barbieri, F. Carvaglios, M. Frigeni and M. Mangano, Nucl. Phys. **B367**, 28 (1993).

TABLES

TABLE I. Cross sections in fb at Tevatron after cuts for cases 1 and 2 of slepton production, along with chargino production and SM backgrounds. We take $\mu = -m_{\tilde{g}}$ and $\tan\beta = 2$. Cuts are described in the text. The bound signifies the 1 event level in our simulations. Results have summed over e 's and μ 's.

process	$m_{\tilde{g}}$	$m_{\tilde{\ell}_L}$	$m_{\tilde{\ell}_R}$	$m_{\tilde{\nu}}$	$m_{\tilde{W}_1}$	$m_{\tilde{Z}_1}$	$\sigma(fb)$
$\tilde{\ell}\tilde{\ell}$ (Case 1)	150	88	80	62	63	24	18
$\tilde{\ell}\tilde{\ell}$ (Case 2)	200	112	102	93	73	32	9
$\tilde{W}_1\tilde{W}_1$ (Case 1)	150	88	80	62	63	24	5
$\tilde{W}_1\tilde{W}_1$ (Case 2)	200	112	102	93	73	32	3
WW	—	—	—	—	—	—	36
$t\bar{t}(150)$	—	—	—	—	—	—	< 1
$Z \rightarrow \tau\bar{\tau}$	—	—	—	—	—	—	< 9

TABLE II. Dilepton cross sections in fb and cut efficiency at LHC after cuts for four cases of slepton production, along with backgrounds from top quark and W-boson pair production. We take $\mu = -m_{\tilde{g}}$ and $\tan\beta = 2$, and $m_t = 150$ GeV. Cuts are described in the text. Results have summed over e 's and μ 's.

cut	case 3	case 4	case 5	case 6	WW	$t\bar{t}$
none	3.5K	243	55	17	100K	1450K
A	431(12%)	46(19%)	10(18%)	3.2(19%)	477(0.5%)	20K(1.4%)
B	62(14%)	22(48%)	6(60%)	2.5(78%)	11(2.3%)	3K(15%)
C	14(22%)	5(23%)	0.8(13%)	0.3(12%)	2(18%)	7.8(0.3%)
D	14(100%)	5(100%)	0.8(100%)	0.3(100%)	2(100%)	7.3(93%)

TABLE III. Cross sections in fb after final $p_T(\ell)$ and $\Delta\phi(\ell\bar{\ell})$ cut along with background at LHC for four cases of slepton production. Parameters are as in Table 2. Results have summed over e 's and μ 's.

case	p_{T_c} (GeV)	$\Delta\phi_c$ (deg)	signal	$t\bar{t}(150)$	WW	$t\bar{t}(1\%)$
case 3	40	90	2.2	0.06	< 0.03	0.33
case 4	40	90	1.3	0.06	< 0.03	0.33
case 4	80	140	0.8	< 0.03	< 0.03	0.09
case 5	80	140	0.22	< 0.03	< 0.03	0.09
case 6	80	140	0.1	< 0.03	< 0.03	0.09

FIGURES

FIG. 1. Slepton masses as a function of $m_{\tilde{g}}$ as given by Eq. 3, for a) $m_{\tilde{q}} = m_{\tilde{g}}$ and b) $m_{\tilde{q}} = 2m_{\tilde{g}}$. We plot for $\tan \beta = 2$ (solid) and 20 (dashes).

FIG. 2. Total cross section for pair production of charged sleptons and sneutrinos via DY mechanism versus slepton mass, for $p\bar{p}$ collisions at $\sqrt{s} = 1.8$ TeV.

The sleptons are taken to be degenerate.

FIG. 3. Total cross section for pair production of charged sleptons and sneutrinos via DY mechanism versus slepton mass, for pp collisions at $\sqrt{s} = 14$ TeV.

The sleptons are taken to be degenerate.

FIG. 4. Distribution in transverse mass for single lepton plus no jet events from sleptons of case 3 and 4, and backgrounds from $W^* \rightarrow \ell\nu_\ell$, WZ and $t\bar{t}$ production, at $\sqrt{s} = 14$ TeV.

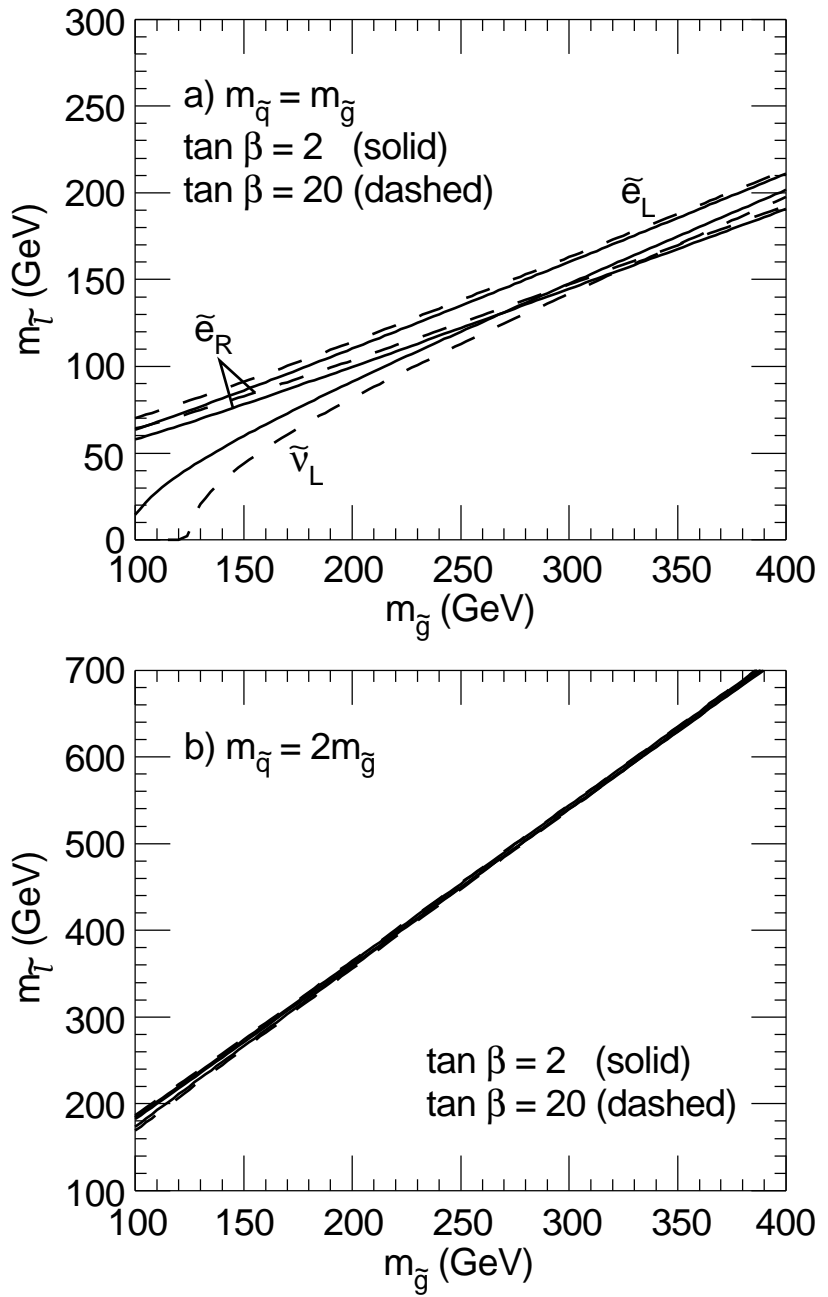


FIG. 1

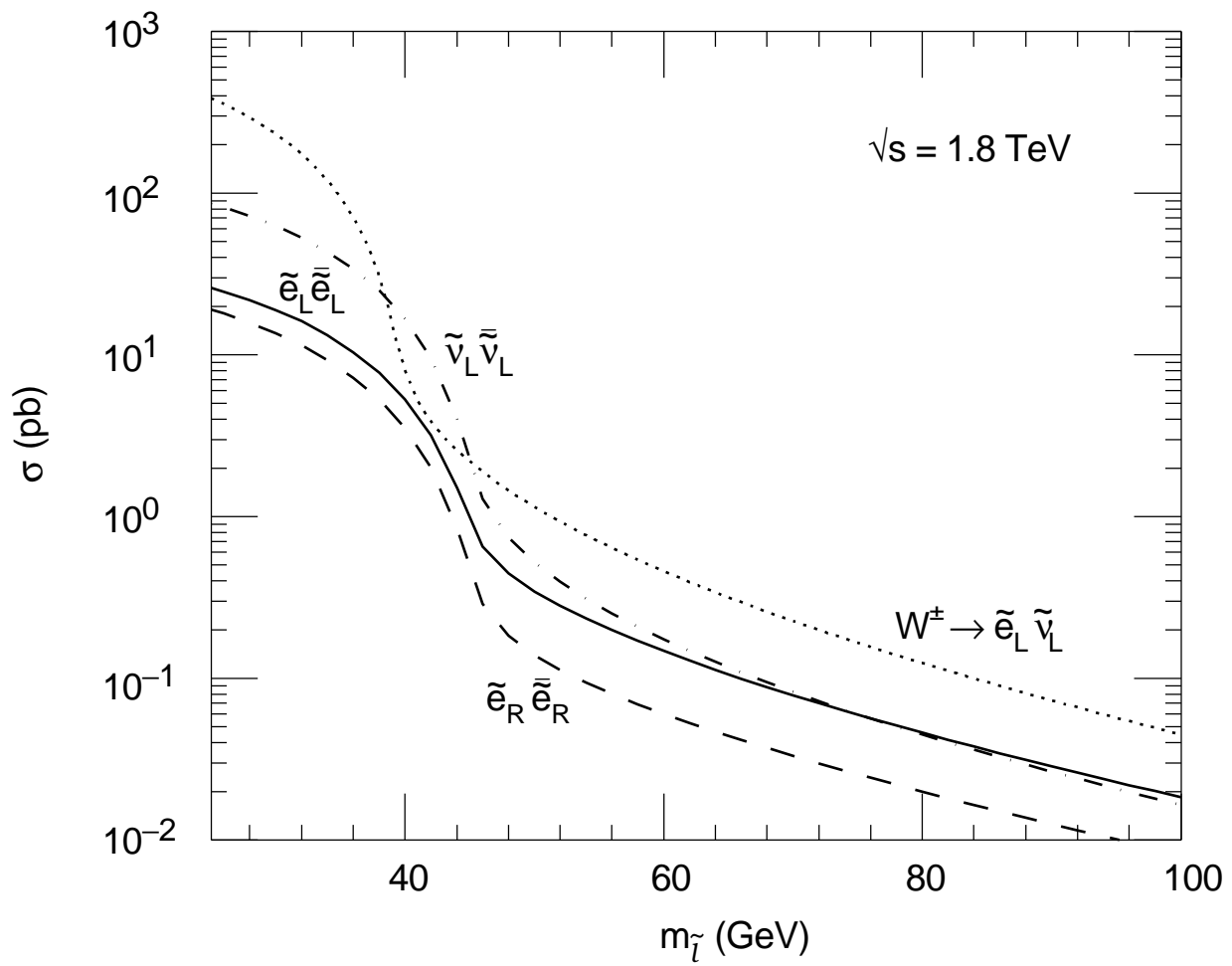


FIG. 2

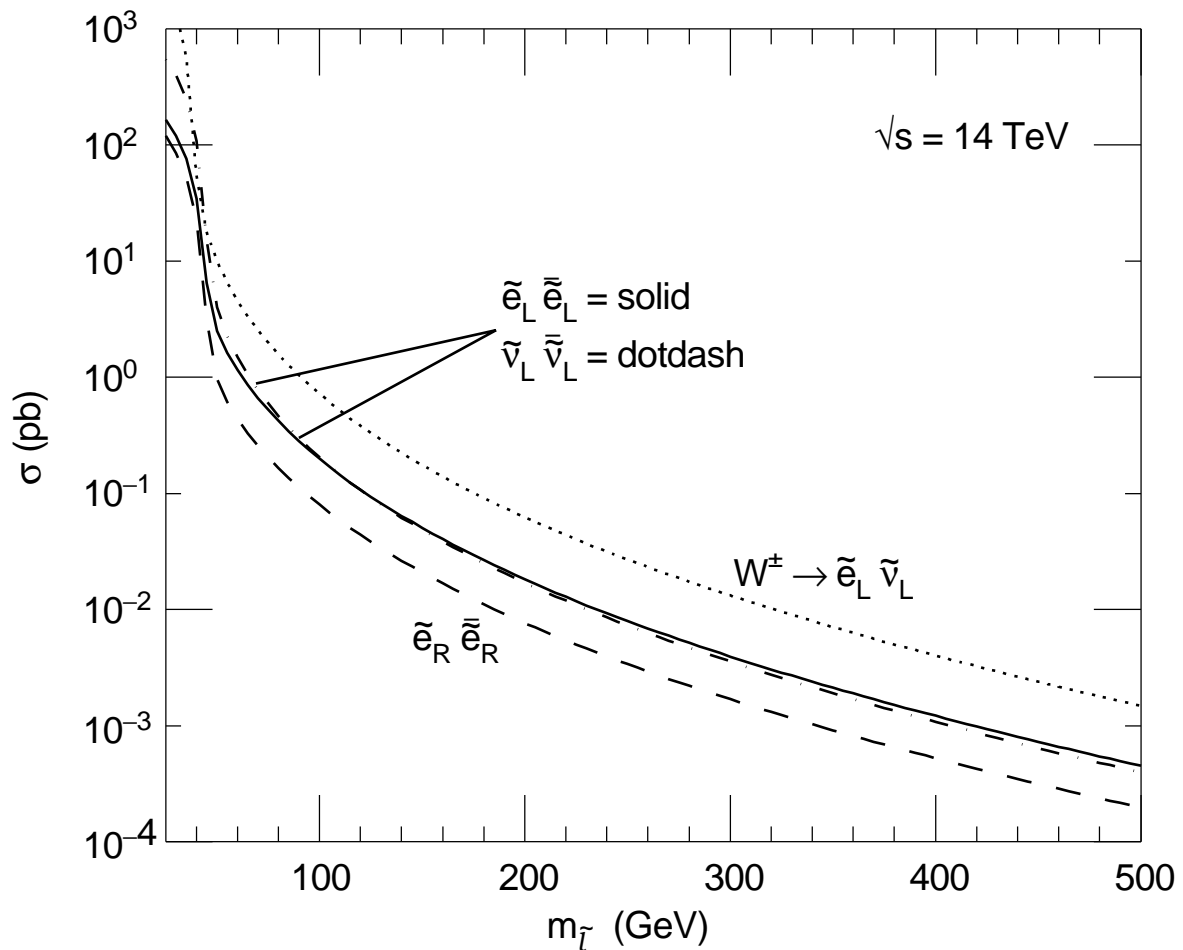


FIG. 3

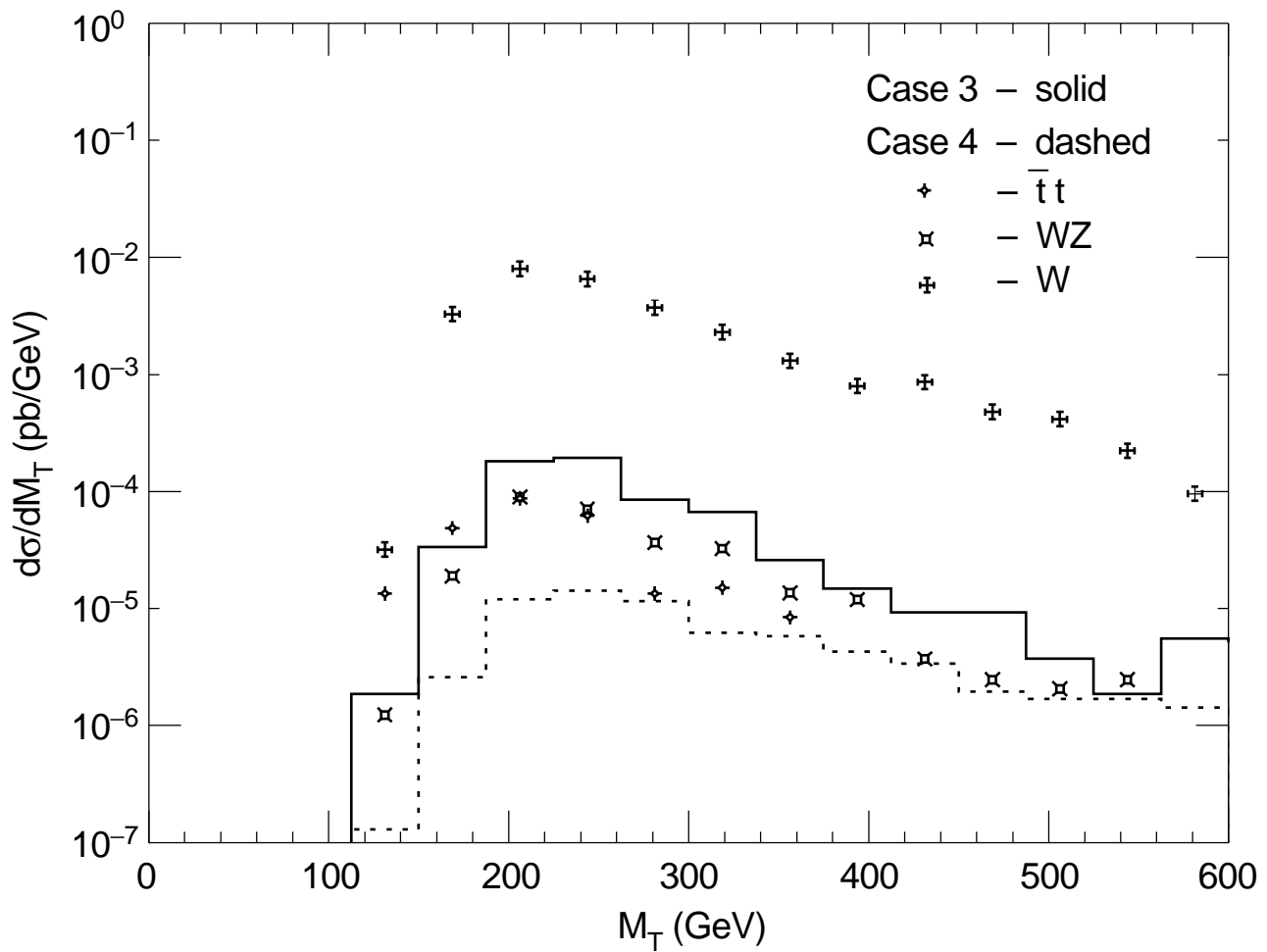


FIG. 4